NJC

Accepted Manuscript

This is an *Accepted Manuscript*, which has been through the Royal Society of Chemistry peer review process and has been accepted for publication.

Accepted Manuscripts are published online shortly after acceptance, before technical editing, formatting and proof reading. Using this free service, authors can make their results available to the community, in citable form, before we publish the edited article. We will replace this *Accepted Manuscript* with the edited and formatted *Advance Article* as soon as it is available.

You can find more information about *Accepted Manuscripts* in the Information for Authors.

Please note that technical editing may introduce minor changes to the text and/or graphics, which may alter content. The journal's standard Terms & Conditions and the Ethical guidelines still apply. In no event shall the Royal Society of Chemistry be held responsible for any errors or omissions in this *Accepted Manuscript* or any consequences arising from the use of any information it contains.

ROYAL SOCIETY OF CHEMISTRY

www.rsc.org/njc

Journal Name

ARTICLE

Facile synthesis of Ag/ZnO micro-flower and improved the ultraviolet and visible light photocatalytic activity

Received 00th January 20xx,
Accepted 00th January 20xx

DOI: 10.1039/x0xx00000x

www.rsc.org/

Yimai Liang[a], Na Guo[a], Linlin Li[a], Ruiqing Li[a], Guijuan Ji[a]* and Shucai Gan[a]*

Three-dimensional (3D) flower-like Ag/ZnO heterostructures with different Ag contents were prepared using a facile two-step method. The samples structure, morphology and optical properties were well-characterized by XRD, SEM, EDS, XPS, DRS, PL, ICP-AES techniques. Results demonstrated the successful deposition of Ag nanoparticles on flower-like ZnO surface. The photocatalytic performance was evaluated by the photocatalytic degradation of Rhodamine B (RhB) under ultraviolet and visible light respectively. The results showed that the Ag/ZnO heterostructures were superior in photocatalytic activity to the pure ZnO samples and the commercial photocatalyst TiO_2 (Degussa, P25). The enhanced photocatalytic activity was attributed to the effectively separation of electron/hole pairs on flower-like ZnO by employing Ag nanoparticles as a conductor. Furthermore, 3D flower-like Ag/ZnO microspheres exhibited good recycling stabilities over several separation cycles in photodegradation.

1. Introduction

With the increasing in discharge of industrial effluents with organic pollutants, tremendous endeavors were made towards the development of new technologies for the clean up of wastewater. As a kind of new technology of treatment pollutants, the photocatalytic oxidation technology is showing the broad application because it can directly eliminate pollution with a high efficiency without causing any additional damage to the environment.[1-3] Metal oxide semiconductor materials, as a photocatalysis, have received intensive attention in this area because their proper band gaps can effectively utilize light energy. Zinc oxide (ZnO), a direct wide band gap energy (3.37eV) semiconductor, is attractive photocatalyst owing to its high photosensitivity, high thermal stability, lower cost, and environmental sustainability.[4, 5] However, the photocatalytic efficiency of ZnO is restricted by two major intrinsic drawbacks. The photo-generated electron–hole pairs recombine rapidly which brings about a low quantum efficiency, which results in the low photocatalytic efficiency of the ZnO structure systems. Another issue is ZnO has a narrow spectral response range, which is only 3–5% of total solar irradiance, since only UV light can be absorbed by pure ZnO.[6]

To conquer this problem, lots of efforts have been investigated to modifie ZnO, such as controlling the morphology of it,[7] implanting metals,[8, 9] doping non-metals[10, 11] and combining ZnO with carbon materials[12, 13] and so on. Among them, noble metal-ZnO mico/nanocomposite materials have been attracted much more attention due to the following two reasons. For one thing, the noble metal can work as electron scavenging centers to allow effective electron-hole pair separation, leading to improved photocatalytic activity.[14] For another, the incident light with wave-length in certain region will be extensively absorbed by the noble metal nanoparticles due to the surface plasmon absorption (SPA) effect, thus the corresponding photoresponding range will be extended and consequently improve the catalytic performance.[15, 16] Among all kinds of noble metal-semiconductor heterostructures, owing to the low cost and non toxicity of Ag relative to other noble metals, Ag-ZnO materials are particularly suitable for industrial applications. Therefore, the Ag/ZnO composite materials have been prepared through a variety of methods. By far, various kinds of synthetic approaches have been realized in fabricating Ag/ZnO composites. For example, Liu et al. prepared Ag nanoparticles (Ag-NPs) decorated ZnO microspheres (ZnO-MSs) heterostructural composites by ultrasonic technology and microwave polyol process.[17] Huang et al. have synthesized the branched Ag-ZnO heterojunction nanostructure using hydrothermal method with high temperature.[18] Liang et al. reported the fabrication porous 3D flower-like Ag/ZnO heterostructural composites by hydrothermal and photo-chemical deposition methods.[9] Deng et al. prepared Ag-nanoparticles decorated ZnO nanosheets-assembled microspheres (Ag-NPs/ZnOs) via solvothermal method.[19] Saoud et al. synthesis the silver (Ag) nano-spheres (NS) supported on zinc oxide (ZnO) nanorods through two step mechanism, using open vessel microwave reactor.[20] Liu et al. have synthesized Ag/ZnO heterostructures based on ZnO nanorod arrays by photoreduction of $AgNO_3$ in the air, water

[a] College of Chemistry, Jilin University, Changchun 130026, P.R. China.
*Corresponding authors: Guijuan Ji; Shucai Gan
E-mail address: juanziji@126.com (G. Ji); gansc@jlu.edu.cn (S. Gan).
Tel: +86 431 88502259.

and water with ethanol.[39] Mohammadzadeh et al. reported ZnO-Ag nanocomposites synthesized using microwave assisted solution combustion method.[21].Despite the successes, the preparation procedure often greatly suffer from problems of high temperature, need for high vacuum, complex with low yields, high cost, requiring the use of toxic and expensive reagents. To develop a simple, fast, and environmentally friendly route to synthesize the Ag-ZnO materials remains an important topic of investigation.

In this work, hierarchically 3D flower-like Ag/ZnO composites were prepared through precipitation method and photochemical deposition technique, which a simple, low-temperature and eco-friendly synthesis way. The morphologies, structures, optical, and photocatalytic properties of the as synthesized samples were investigated by different techniques. The photodegradation of RhB was used to evaluate the photocatalytic performance of the materials. Results show that the surface modification of ZnO by silver nanoparticles causes improvement in the photocatalytic activity both under UV and visible light irradiation. This surface modification induces an increase of the absorption properties of visible light. And a possible mechanism of photocatalysis under UV and visible light was also discussed and proposed.

2. Experimental

2.1. Materials

Zinc acetate dihydrate ($Zn(CH_3COO)_2$ $2H_2O$), sodium hydroxide (NaOH) and silver nitrate ($AgNO_3$), were purchased from Tianjin Chemical Reagent Research Company. Polyvinylpyrrolidone (PVP) was purchased from Sinopharm Chemical Reagent Research Co. Ltd., China. All chemicals were of analytical grade and were used directly without further purification. Distilled water was used in all experiments.

2.2. Synthesis of 3D flower-like ZnO

The 3D flower-like ZnO heterostructures were fabricated via a simple precipitation method. In a typical synthesis, firstly, 20 mL of distilled water was heated in a beaker to reach a constant temperature of 60 ^{o}C. Then, 200 mL of aqueous PVP solution (12.5 mg/mL) and subsequently 20 mL of zinc acetate (0.10 mol/L) were added at 60 ^{o}C. After the solutions were stirred for 1 min, 20 mL of NaOH (0.50 mol/L) was introduced to the above solutions stirred continuously for 1 h at 60 ^{o}C. Finally, the white precipitation was centrifuged and washed with ethanol and distilled water in sequence several times, followed by drying 60 ^{o}C for 12 h.

2.3. Synthesis of 3D flower-like Ag/ZnO heterostructure composites

A photoreduction method was used to decorate Ag nanoparticles onto the surface of the as prepared 3D flower-like ZnO. In detail, 0.3 g of the flower-like ZnO powder was dispersed in 300 mL $AgNO_3$ aqueous solution, and stirring for 0.5 h to achieve the adsorption of Ag+ ions onto the surface of flower-like ZnO. The obtained suspension was irradiated for 2 h under radiation with continuously stirring by employing a high-pressure Hg UV lamp (GGZ175, 175 W) to reduce Ag+ to zerovalent Ag. The precipitate was separated from the reaction solution by centrifugation, washed with ethanol and rinsed with distilled water and dried in vacuum at 60 °C for 6 h. A series of 3D flower-like Ag/ZnO composites were obtained by a similar procedure, except for different amount of $AgNO_3$. The molar ratio of $AgNO_3/Zn(NO_3)_2$ was changed in the range from 0 to 7% and the products were denoted as ZnO, AZ-1%, AZ-3%, AZ-5%, and AZ-7% respectively, in which the last number corresponds to the molar ratio of $AgNO_3/Zn(NO_3)_2$.

2.4. Characterization

X-ray diffraction (XRD) analysis of porous flower-like ZnO and Ag/ZnO were performed using a D/Max-IIIC (Rigaku, Japan) with Cu Kα radiation. The morphology and dimension of the products were characterized by S-4800 field emission scanning electron microscope (FE-SEM, Hitachi, Japan) with an acceleration voltage of 3 kV. The chemical composition was examined by using energy dispersive spectroscopy (EDS), attached with FESEM. X-ray photoelectron spectroscopy (XPS) analysis was performed on a PHI-5000CESCA system with Mg Kα radiation (hv = 1253.6 eV). The X-ray anode was run at 250 W, and the high voltage was kept at 14.0 kV with a detection angle at 540. All the binding energies were calibrated by using the containment carbon (C 1s = 284.6 eV). UV–vis spectrophotometry (UV-2000, Shmadzu, Japan) was used to measure the optical absorption edge of the samples over the wavelength range of 200 to 800 nm. The photoluminescence spectra (PL) of 3D flower-like Ag/ZnO were recorded using a Hitachi F-7000 spectrophotometer equipped with a 150 W xenon lamp at 343 nm excitation wavelength. The actual content of Ag-NPs was determined using inductively coupled plasma-atomic emission spectrometry (ICP-AES; 7500ce, Agilent Corporation). All measurements were performed at room temperature.

2.5. Photocatalytic experiments

The photocatalytic performance of Ag/ZnO heterostructure was evaluated by using RhB as presentative dye pollutant. A high-pressure Hg UV lamp (GGZ175, 175 W) with a maximum emissionat 365 nm served as the UV light resource. A 500 W Xenon lamp (CEL-HXF300) was used as the visible light source with a 400 nm cut-off filter. In a typical procedure, the 0.04 g catalyst (Ag/ZnO, Degussa P25 and ZnO) was dispersed into 20 mL aqueous solution of RhB (8 mg/L). After stirring in the dark for 0.5 h, the suspensions were placed under light irradiation. During the photoreaction, the samples were collected at regular intervals and centrifuged to remove the catalyst. The concentration of target organic solution before and after degradation was measured by using a UV–vis spectrometer (UV-2550, Shimadzu, Japan).

2.6 Determination of •OH radicals

The formation of hydroxyl radicals (•OH) on the surface of photo-illuminated Ag/ZnO was detected by the photoluminescence (PL) technique using coumarin as a probe molecule, which readily reacts with •OH to produce highly fluorescent product, 7-hydroxycoumarin. The method relies on the PL signal at 460 nm of 7-hydroxycoumarin. The PL intensity of 7-hydroxycoumarin is proportional to the amount of •OH

produced on the surface of Ag/ZnO. Experimental procedures were as follows: 200mg of the prepared AZ-5% sample was added to 200mL of the 10^{-3} M coumarin aqueous solution, and then UV light irradiation of the solution was started. A high-pressure Hg UV lamp (GGZ175, 175 W) with a maximum emissionat 365 nm served as the UV light resource. Sampling was performed in every 30min. Solution after filtration was analyzed on a Hitachi F-4500 fluorescence spectrophotometer. The product of coumarin hydroxylation, 7-hydroxycoumarin, gave a peak at the wavelength of about 460nm by the excitation with the wavelength of 332 nm.

3. Results and discussion

3.1. Morphological and structural analysis

The phase characters of the prepared samples were studied by X-ray diffraction (XRD). As shown in Fig. 1, it can be found that pure ZnO sample had sharp peaks at 31.78°, 34.42°, 36.28°, 47.56°, 56.62°, 62.86°, 67.96°, 69.10°. The positions of all the peaks can be indexed to the wurtzite ZnO structure (JCPDS No. 36-1451) and correspond to (100), (002), (101), (102), (110), (103), (112) and (201), respectively. For those Ag decorated samples, four additional peaks at 38.14°, 44.26°, 64.42° and 77.44°, which were readily assigned to the (111), (200), (220) and (311) planes of face center cubic (fcc) Ag peaks (JCPDS No. 04-0783), respectively. Additionally, the peak intensity of Ag phase gradually increases due to the increasing amount of Ag nanostructure in the Ag/ZnO composites, and no peaks of any other phases or impurities are observed from the XRD patterns, which indicate the high purity of the samples. These results further confirm that Ag/ZnO composites were made up of ZnO and Ag phases and no other phases.

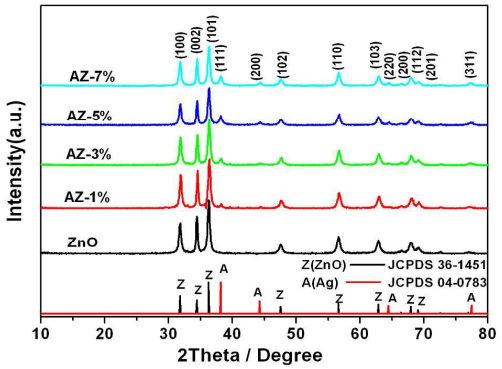

Fig. 1 XRD patterns of the as-prepared ZnO and the Ag/ZnO composites with different Ag contents.

In order to investigate the morphologies of as-prepared ZnO, Ag/ZnO composites, SEM observation was carried out. Fig. 2a, b are typical SEM images of the as-synthesized ZnO. It can be seen clearly that the ZnO shows well-defined 3D flower-like hierarchical structures with good monodispersity. The average size of these flower-like structures is about 1μm. The morphology of the AZ-1%, AZ-3%, AZ-5%, AZ-7% samples are shown in Fig. 2c-f respectively. It can be noted that the Ag/ZnO particles remained 3D flower-like structure, and a tailored amount of Ag nanoparticles with an average diameter of 60 nm were observed on the surfaces of ZnO flowers. With the increase of the deposition amount of Ag on ZnO, there are increasing nanoparticles of Ag growing on the surfaces of the ZnO flowers, and the surfaces become coarse compared with those of single ZnO hierarchical structure. To investigate the real amount of Ag-NP, elemental analysis of the as-prepared samples was performed using ICP-AES. Table 1 presents the theoretical percentage of Ag added ($Ag_{theoretical}$/wt %) and the real percentage of Ag supported on the ZnO structure (Ag_{real}/wt %). Additionally, the real atomic/molar ratio of Ag/ZnO was calculated, resulting in values of 0.82, 2.72, 4.40 and 6.26 atom % for the theoretical depositing amount of 1, 3, 5 and 7 atom %, respectively.

Sample	$Ag_{theoretical}$/wt % (Ag/(Ag+ZnO))	Ag_{real}/wt % (Ag/(Ag+ZnO))	Atom % (Ag/ZnO)
ZnO	0	0	0
AZ-1%	1.30	1.05	0.82
AZ-3%	4.00	3.62	2.72
AZ-5%	6.68	5.87	4.40
AZ-7%	9.32	8.34	6.26

Table 1 Experimental weight percentage obtained by ICP–AES and atomic/molar percentage compared to the theoretical, stoichiometric weight percentage.

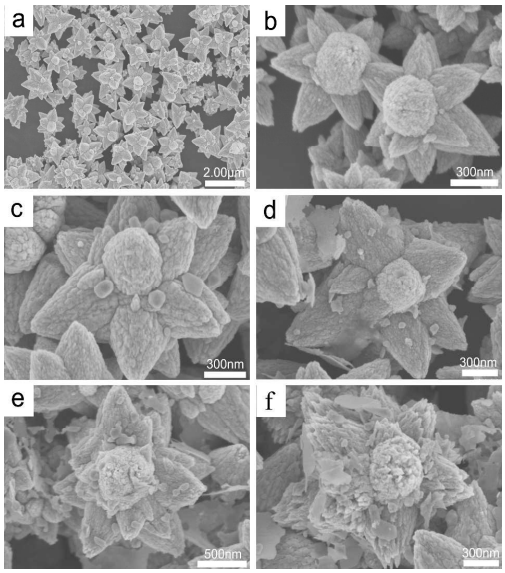

Fig. 2 SEM images for (a, b) as prepared 3D flower-like ZnO, (c) AZ-1%, (d) AZ-3%, (e) AZ-5%, (f) AZ-7%.

The structure of the product was further examined by the TEM image. Fig. 3 shows the typical TEM image of as-synthesized flower-like AZ-5% sample. It revealed a unique flower-shaped morphology of ZnO, and Ag nanopaticles are well decorated on the surface of flowers. The TEM image of as-synthesized AZ-5% sample depicts full consistency with the observed SEM results. To further characterize the as-prepared samples, the elemental composition of Ag/ZnO composites were examined by energy dispersive spectroscopy (EDS) attached with FESEM. Fig. 4a, c depicts the typical FESEM image of as-prepared AZ-

5% sample. It can be seen clearly that the AZ-5% composites exhibits a well 3D flower-like hierarchical structure. Fig. 4b shows EDS spectrum of AZ-5% sample while the Fig. 4d-f depict the corresponding elemental mapping for Zn, O and Ag. The result confirms that the AZ-5% samples are only composed of Zn, O and Ag elements, which is consistent with the XRD results. In a summary, Ag has been successfully deposited on the surface of 3D flower-like ZnO and the presence of Ag does not destroy such flower-like structure. Thus, the elemental mapping further confirmed that the synthesized 3D flower-like Ag/ZnO composites.

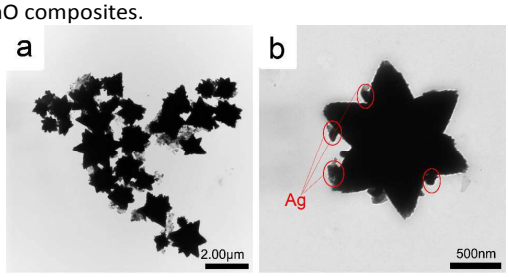

Fig. 3 TEM images of the as-prepared AZ-5% samples.

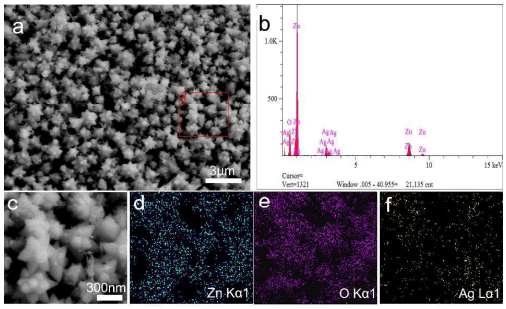

Fig. 4 (a, c) FESEM image of the as-prepared AZ-5% samples, (b) EDS spectrum of AZ-5% sample and its corresponding elemental mapping images for (b) zinc, (e) oxygen and (f) silver.

3.2. XPS analysis

The surface chemical composition and valence state of the as-prepared ZnO and AZ-5% samples were investigated by XPS analysis, and the corresponding results are shown in Fig. 5. Fig. 5a shows the full scan XPS spectra of the 3D flower-like ZnO and AZ-5% samples. There are only C, Zn, and O element peaks in the pure ZnO sample. An additional Ag peak is observed in heterostructured Ag-ZnO composites. The presence of C might be caused by the XPS instrument. No any other peaks can be observed. This result confirms that the ZnO is composed only with two elements, Zn, O, and AZ-5% samples is formed by Zn, O, and Ag, which is consistent with the XRD and EDS results discussed above. High-resolution spectra of Zn, O and Ag species obtained from the sample are shown in Fig. 5b-d, respectively. It can be found that compared to pure ZnO sample, there are positive shifts of Zn and O binding energy in AZ-5%. The high-resolution Zn 2p spectrum is shown in Fig. 5b, the peaks of AZ-5% with binding energy near 1045.2 and 1022.1eV could be attributed to $Zn2p_{1/2}$ and $Zn2p_{3/2}$, which confirms that Zn element exists mainly in the form of Zn^{2+}.[22] In Fig. 4c, the asymmetric spectra of the O 1s can be fitted into two symmetrical peaks of AZ-5% (locating near 530.3 eV and 531.9 eV, respecively), which implies two different kinds of O species in the sample. They should be associated with the lattice oxygen of ZnO and chemisorbed oxygen of the surface hydroxyls, respectively.[23] Furthermore, the binding energies of Ag 3d for AZ-5% shift to the lower binding energy compared with bare Ag (368.2 and 374.2 eV for Ag $3d_{5/2}$ and Ag $3d_{3/2}$, respectively).[24] When Ag nanopaticles are in situ deposited onto the ZnO samples, the positions of their corresponding Fermi energy levels need to adjust to the same value. Therefore, there are some free electrons above the new Fermi level of Ag nanopaticles, which could return to the conduction band of ZnO, resulting in the tendency of Ag to higher valence. Because the binding energy of oxidation state Ag^{+} is lower than that of substance Ag (Ag is a kind of transition metal), the peaks of Ag 3d in Ag/ZnO heterostructure shift obviously.[25] For 3D flower-like AZ-5% sample, the positive shift of Zn, O and the negative shift of Ag are due to the interaction between Ag nanoparticle and ZnO, which similar results are also found in the previous work.[26, 27]

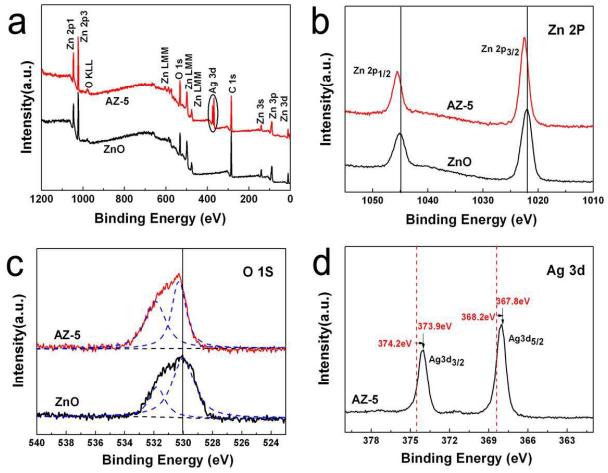

Fig. 5 XPS spectra of ZnO and AZ-5% samples: (a) The survey scan spectrum; (b) Zn 2p spectrum; (c) O 1s spectrum and (d) Ag 3d spectrum.

3.3. UV–vis diffuse reflectance spectra

Electronic spectra of photocatalysts could remarkably affect their photocatalytic activities. Hence, the spectra of the as-prepared samples were examined using DRS technique and the results are shown in Fig. 6. For all samples, strong absorption edges observed about 368 nm is assigned to ZnO semiconductor. Bare 3D flower-like ZnO showed absorption in UV-region without any absorption in the visible range. Compared to pure ZnO, the Ag/ZnO composites exhibited a red shift in absorption more intense absorption in the visible region, which is attributed to the surface plasmon resonance effect of silver.[28] Because the surface plasmon resonance of Ag nanoparticles on the ZnO is excited by visible light, the photocatalytic activity of ZnO can be distinctly enhanced. The increase in absorbance in the visible region can be observed by

adding Ag and the absorption intensity of AZ-5% was the highest one. This enhancement in the optical absorption is caused by the increase of defect sites in the catalyst crystal structure which can inhibit the recombination of the charge carriers and enhances the photocatalytic activity of the catalyst.[29] The UV absorption edge was red-shifted with Ag doping, indicating a reduction in the band gap. The same result is obtained with T. J. Whang et al..[30]

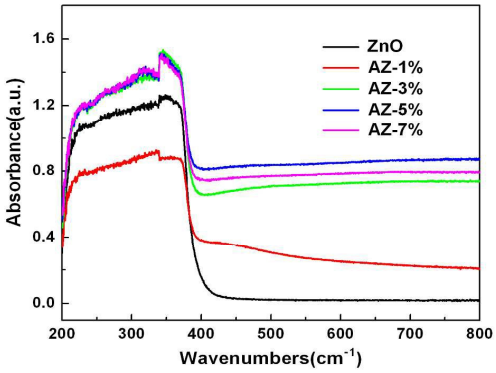

Fig. 6 UV–vis diffuse reflectance spectra of 3D flower-like ZnO, AZ-1%, AZ-3%, AZ-5%, AZ-7%.

3.4. Photoluminescence spectra (PL)

In photocatalytic process, the separation and recombination of photogenerated electrons–holes are two competitive processes, and photocatalytic activity is closely related to the lifetime of photogenerated electrons and holes.[31] The photoluminescence (PL) spectra of the samples were evaluated to investigate the electronic, optical and photochemical properties of photocatalysts, from which the efficiency of charge carrier trapping, immigration and transfer can be evaluated.[32] Fig. 7 is the room temperature PL spectra of as-prepared ZnO and Ag/ZnO composites with various Ag contents. The excitation wavelength is 340nm, which was determined from the emission spectra. It can be seen that all samples exhibit a narrow UV peak centered at about 387 nm, corresponding to the ultraviolet emission of ZnO particles. From PL spectra, we can found that the PL intensity decrease after the deposition of Ag on the ZnO surface, indicating that Ag nanopaticles on ZnO surface can the inhibit the recombination of electron–hole pairs. Moreover, it can be seen clearly that PL emission intensity first decreases and then increases with the increase of Ag content.[33] The AZ-5% sample shows the minimum PL intensity. When the amount of Ag increased further, up to 7%, the intensity of the spectra increased, and indicated that the recombination of the electrons and holes increased. The increase of the recombination of electrons and holes may be attributed to the aggregation of Ag nanoparticles in the composites, which act as the recombination centers, and consequently, increase the charge recombination.[34] The charge separation and recombination impose a direct impact on the photocatalytic activity of the catalyst.

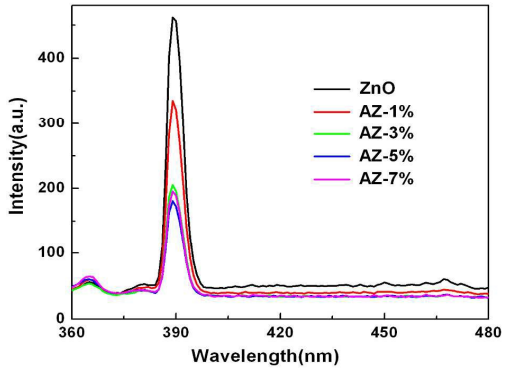

Fig. 7 PL spectra of 3D flower-like ZnO, AZ-1%, AZ-3%, AZ-5%, AZ-7% samples.

3.5 Photocatalytic performance

To investigate the photocatalytic activity of Ag/ZnO samples, RhB was used as a model pollutant for UV and visible light irradiation, respectively. Fig. 8 a and b show the degradation rate of RhB in the presence of different catalysts (Ag/ZnO, ZnO and P25) under UV and visible light illumination, respectively. In Fig. 8a and b, the relative concentration C/C_0 of RhB in solution was plotted as a percentage against UV or visible light irradiation time for the catalysts, where C was the concentration of RhB remaining in the solution after irradiation time t, and C_0 is the initial concentration of the RhB.

From Fig. 8a, there was no RhB degradation in the absence of a photocatalyst (the blank) after 180 min of UV irradiation. Compared to pure ZnO and P25, all Ag/ZnO samples exhibited an increase in the UV driven RhB degradation rate, indicating that loaded Ag on ZnO is an effective way to improve photocatalytic performance. The content of Ag in the composites has obvious influence on the photocatalytic activity. As shown in Fig. 8a, the photodegradation efficiency of RhB is about 27%, 30%, 68%, 79%, 100% and 82% for P25, ZnO, AZ-1%, AZ-3%, AZ-5% and AZ-7% respectively, when the reaction was performed under UV-light for 180 min. The results indicate that Ag/ZnO composites are superior to P25 for photodegradation of RhB dye. We can see that the activity of Ag/ZnO composites firstly increased and then decreased with the increase of Ag amount in the composites. The AZ-5% sample exhibits the highest photodegradation rate. The deposition of Ag nanoparticles with appropriate amount on ZnO surface can effectively trap and transfer the photogenerated electrons, and thus reduce the recombination of the electro-hole pairs. However, excessive Ag was used, the aggregation and/or size increase of the Ag particles will happen, which is disadvantageous to inhibit the recombination of the electron-hole pairs.[35, 36]

The visible-light-responsive property of 3D flower-like Ag/ZnO composites was further examined. Fig. 8b shows the photodegradation of RhB by different catalysts under visible light irradiation. It can be seen that no significant degradation of RhB in the pure ZnO and P25 samples due to ZnO and TiO_2 with wide band gap energy. Comparing with the pure ZnO, all Ag/ZnO heterostructures samples exhibit much higher photocatalytic activities. Among these catalysts, the AZ-5%

sample exhibited the highest photocatalytic activities. These results follow a trend similar to that of the UV–vis diffuse reflectance spectra (Fig. 6) results. For pure ZnO, it has no absorption in the visible region and no photocatalytic activity under the visible light. However, due to the surface plasmon resonance of Ag nanoparticles, most photogenerated electrons may be excited from the surfaces of Ag nanoparticles to the conduction band of ZnO and then diffuse to the surrounding medium to promote photocatalysis. Generally, Ag depositing can modify the electronic properties of ZnO, leading to the optical absorption of ZnO extend to the visible light region.[37] This provides a facile and efficient pathway for the photocatalytic degradation of RhB in the visible-light region. Similar results were also found by some other works.[38, 39]

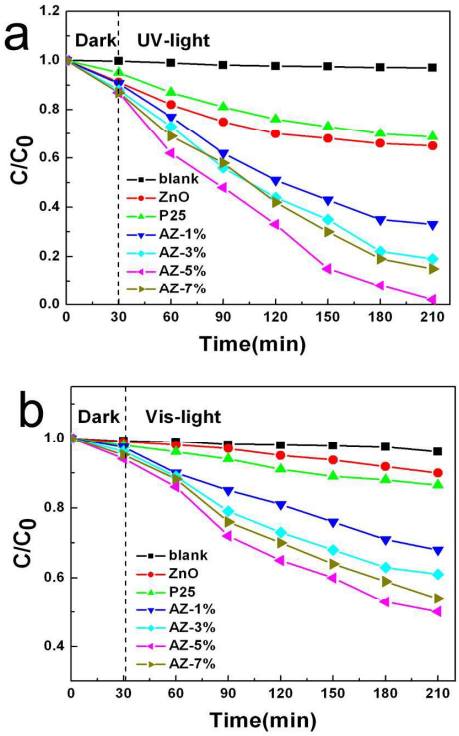

Fig. 8 Photodegradation curves of RhB by different catalysts under (a) UV and (b) Visible light irradiation.

The possible process of photoexcitation and charge transfer for Ag/ZnO photocatalyst under UV and visible light irradiation has been proposed and is shown in Fig. 9. When the Ag/ZnO heterostructure is illuminated with UV light with photon energy higher or equal to the band gap of ZnO, electrons in the valence band (VB) can be excited to the conduction band (CB) leaving the corresponding holes in the VB (Eq. (1)). For pure ZnO, these photogenerated electrons and holes are easy to recombine within a time scale of nanoseconds. For the Ag/ZnO nanocomposites, as it is shown in Fig. 9(a), the bottom energy level of the conduction band (CB) of ZnO is higher than the equilibrium Fermi energy level (E_f) of Ag/ZnO heterostructure, so photoexcited electrons will transfer from ZnO particles to Ag particles driven by the potential energy. It has been proposed that a Schottky barrier formed at the interface between metal and semiconductor, while the holes can remain on the semiconductor surfaces.[40] Furthermore, Ag particles or clusters on the surface of ZnO particles described as a sink, and they not only reduce the recombination of photoinduced electrons and holes but also prolong the lifetime of photogenerated pairs. Subsequently, the transferred electrons can be easily trapped by the adsorbed O_2 molecules to produce $\bullet O_2^-$ (Eq. (2)). The photo-induced holes in ZnO can be scavenged by the immanence H_2O molecules to yield •OH (Eq. (3)). These •OH are reactive oxidative species, which will attack the RhB molecules and subsequently decompose them into CO_2 and H_2O (Eq. (4)).[41, 42] This process can be proposed as follows.

$$ZnO + h\nu \rightarrow ZnO(e^- + h^+) \quad (1)$$

$$e_{cb}^- + O_2 \rightarrow \bullet O_2^- \quad (2)$$

$$h_{vb}^+ + OH \rightarrow \bullet OH \quad (3)$$

$$\bullet OH + RhB \rightarrow degradation\ product \quad (4)$$

When they are illuminated by visible light (Fig. 9(b)), ZnO cannot be excited and its Fermi level is kept unchanged. However, due to the surface plasmon resonance (SPR) of Ag nanoparticles, most photogenerated electrons may be excited from the surfaces of Ag nanoparticles to the conduction band of ZnO, which will facilitate the formation of hydroxyl radicals and subsequently enhance the visible light photocatalysis.[43] This may serve to understand the improved catalytic performance of Ag/ZnO under visible light irradiation.

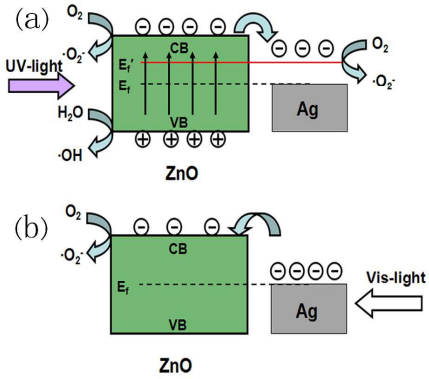

Fig. 9 Schematic diagram of electron transfer of Ag/ZnO heterostructures under (a) UV light irradiation and (b) Visible light irradiation.

In Ag/ZnO photocatalysis, active oxygen species such as hydroxyl radical (•OH) and superoxide radical ($\bullet O_2^-$) have been regarded as the key species during the photocatalytic oxidation reaction. Among these highly oxidative species, the hydroxyl radical (•OH) has long been assumed to be the major species for mineralization of pollutants either adsorbed on the Ag/ZnO surface or in the bulk solution.[44] In order to detect the hydroxyl radicals (•OH) formed on the surface of photo-

illuminated Ag/ZnO, the fluorescence technology was applied. The method is rapid, sensitive, and specific, which only needs simple standard PL instrumentation. Coumarin reacts with •OH readily to produce a highly fluorescent product, 7-hydroxycoumarin, whose PL peak intensity is in proportion to the amount of •OH radicals produced in water. Experimental procedures were reported in earlier reports. [45, 46] Experimental procedures were as follows: 200mg of the prepared Ag/ZnO sample was added to 200mL of the 10^{-3} M coumarin aqueous solution, and then UV light irradiation of the solution was started. A high-pressure Hg UV lamp (GGZ175, 175 W) with a maximum emissionat 365 nm served as the UV light resource. Sampling was performed in every 30min. Solution after filtration was analyzed on a Hitachi F-4500 fluorescence spectrophotometer. The 7-hydroxycoumarin was scanned with an excitation at 332 nm. Fig. 10 shows the changes of PL spectra of coumarin solution with UV-light irradiation time. A gradual increase in PL intensity at about 460 nm is observed with increasing irradiation time. The •OH radical determination reaction using AZ-5% sample photocatalysts were performed, and the results are shown in Figure 10. The result reveals that in the photocatalytic system fluorescence intensity is increased with increase in the irradiation time. This finding indicates that the occurrence of fluorescence can be ascribed to the chemical reactions between the probe molecules and the hydroxyl radicals formed on the AZ-5% surface via photocatalytic reaction. It is suggested that •OH radicals are formed in the photocatalytic degradation reaction, which agrees well with the results of the discussion of photocatalytic mechanism.

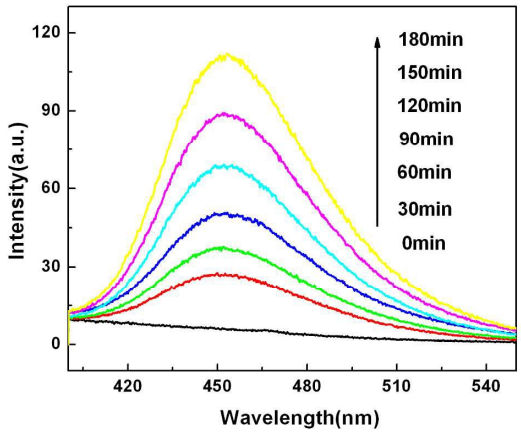

Fig. 10 PL spectral changes observed during illumination of AZ-5% dispersed in a 10^{-3}M coumarin aqueous solution acid (excitation at 332nm). Each fluorescence spectrum was recorded every 30 min of UV light illumination.

To evaluate the stability of photocatalytic performance in UV light irradiation, the AZ-5% was used to degrade RhB dye in three repeated cycles, and the results are shown in Fig. 11(a). After three-times recycling, the photocatalytic efficiency of this catalyst only display a little drop, confirming that Ag/ZnO heterostructure possesses a favorable ability to repetitively photodegradate RhB in the aqueous solution upon UV irradiation. Furthermore, the cycling performance of the sample AZ-5% was also investigated in visible light irradiation, and the results are shown in Fig. 11(b). It also can be seen that after three cycles, the photocatalytic performance shows just a little decreasing. It clearly demonstrates that Ag/ZnO heterostructure also have a good stability of photocatalytic performance in visible light irradiation.

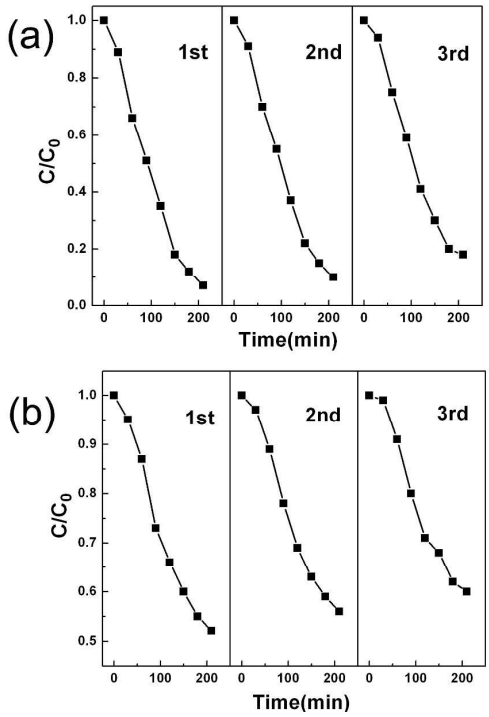

Fig. 11 Three photocatalytic degradation cycles of RhB using AZ-5% under UV(a) and Visible (b) light irradiation.

4. Conclusions

In summary, we successfully synthesized 3D flower-like Ag/ZnO using a facile two-step method. The formation of Ag/ZnO composites owe to a strong interfacial interaction between ZnO micro-flower and Ag nanoparticles. Similar reports were observed by some previous literatures. [47-49] The influence of the Ag depositing on the structures, optical, and photocatalytic properties of the synthesized the ZnO samples has been investigated in detail. Results indicate that light absorption extends to the visible region for Ag/ZnO, and the electron-hole recombination can be effectively inhibited. The as-prepared Ag/ZnO samples had shown significant enhanced photocatalytic activity toward RhB degradation under UV and visible-light irradiation. The enhanced photocatalytic activity could be attributed to the decorated Ag nanoparticles on ZnO. The Ag nanoparticles deposited on the ZnO surface act as the electron wells to promote the charge separation and the surface plasmatic effect of the deposited Ag nanoparticles enhance the photocatalytic performance in visible region.

Moreover, Ag/ZnO photocatalyst can remain its good photocatalytic performance after three cycles, making it a promising candidate as highly efficient photocatalyst for pollutant removal.

Acknowledgements

This work was supported by the Mineral and Ore Resources Comprehensive Utilization of Advanced Technology Popularization and Practical Research (MORCUATPPR) founded by the China Geological Survey (grant no. 12120113088300). It was also supported by the Key Technology and Equipment of Efficient Utilization of Oil Shale Resources (no. OSR-05) and the National Science and Technology Major Projects (no. 2008ZX05018).

References

1 C. C. Chen, W. H. Ma and J. C. Zhao, *Chem. Soc. Rev.*, 2010, **39**, 4206.
2 H. Tada, T. Kiyonaga and S. Naya, *Chem. Soc. Rev.*, 2009, **38**, 1849.
3 K. Pandiselv iand S. Thambidurai, *Colloids. Surfaces. B.*, 2013,**108**, 229.
4 Y. L. Fang, Z. Y. Li, S. Xu, D. D. Han and D. Y. Lu, *J. Alloy. Compd.,* 2013, **575**, 359.
5 Y. Y. Sun ,L. Jiang and X. S. Sun, *New J. Chem.*, 2015, **39**, 2943.
6 J. Manna, S. Goswami, N. Shilpa and N. Sahu, *ACS Appl. Mater. Interfaces.*, 2015, **7**, 8076.
7 M. S. Wang, Y. P. Zhang, Y. J. Zhou, F. W. Yang and S. G. Seong, *CrystEngComm*, 2013, **15**, 754.
8 M. Misra and P. Kapur, *New J. Chem.*, 2014, **38**, 4197.
9 Y. M. Liang, N. Guo, L. L. Li, R. Q. Li, G. J. Ji and S. C. Gan, *Appl. Surf. Sci.*,2015, **332**, 32.
10 D. M. Chena, K.W. Wang, W. Q. Yao and Y. F. Zhu, *Appl. Catal. B-Environ.,* 2014, **147**, 554.
11 B. Subash, A. Senthilraja, P. Dhatshanamurthi and M. Shanthi, *Spectrochimica Acta Part A: Molecular and Biomolecular Spectroscopy,* 2013, **115** ,175.
12 H. Fu, T. Xu, S. Zhu and Y. Zhu, *Environ. Sci. Technol.,* 2008, **12**, 8064.
13 J. B. Mu, C. L. Shao, Z. C. Guo, Z. Y. Zhang, M. Y. Zhang, P. Zhang and B. Chen, *ACS Appl. Mater. Interfaces*, 2011, **3**, 590.
14 C. Mondal, J. Pal, M. Ganguly and T. Pal, *New J. Chem.*, 2014, **38**, 2999.
15 H. M. S. Suh, J. R. Choi, H. J. Hah, S. M. Koo and Y. C. Bae, *J. Photoch. Photobiolo. A.,* 2004, **163**, 37.
16 Q. Zhang, J. K. Liu, J. D. Wang and H. X. Luo, *Ind. Eng. Chem. Res.*, 2014, **53**, 13236.
17 H. R. Liu, Y.C. Hua, Z. X. Zhang and H. S. Jia, *Appl. Surf. Sci.*, 2015, **355**, 644.
18 Q. L. Huang, Q. T. Zhang and S. S. Yuan, *Appl. Surf. Sci.*, 2015, **353**, 949.
19 Q. Deng, H. B. Tang, G. Liu, X. P. Song and G. P. Xua, *Appl. Surf. Sci.*, 2015, **331**, 50.
20 K. Saoud, R. Alsoubaihi, N. Bensala, T. Bora and M. Bertino, *Mater. Res. Bull.*, 2015, **63** 134.
21 S. Mohammadzadeh and M. E. Olya, *J. Environ Sci.*, 2015, **35**, 194.
22 P. Chen, L. Gu, X. D. Xue and Y. Y. Song, *Mater. Chem. Phys.*, 2010, **122**, 41.
23 S. M. Hosseini, I. A. Sarsari, P. Kameli and H. Salamati, *J. Alloy. Compd.*, 2015, **640**, 408.
24 C. D. Gu, C. Cheng, H. Y. Huang, T. L. Wong, N. Wang and T. Y. Zhang, *Cryst. Growth., Des.* 2009, **9**, 3278.
25 W. W. Lu, S. Y. Gao and J. J. Wang, *J. Phys. Chem. C.,* 2008, **112**, 16792.
26 Z. Z. Han, L. L. Ren, Z. H. Cui and J. Z. Chen, *Appl. Catal. B-Environ.,* 2012, **126**, 298.
27 X. Q. Liu, Z. Li, W. Zhao, C. X. Zhao, J. B. Yang and Y. Wang, *J. Colloid. Interf. Sci.*, 2014, **432**, 170.
28 M. K. Lee, T. G. Kim, W. Kim and Y. M. Sung, *J. Phys. Chem. C.*, 2008, **112**, 10079.
29 O. Bechambia, M. Chalbib and W. Najjara, *Appl. Surf. Sci.*, 2015, **347**, 414.
30 T. J. Whang, M. T. Hsieh and H. H. Chen, *Appl. Surf. Sci.*, 2012, **258**, 2796.
31 Y. M. Liang, N. Guo, G. J. Ji and S. C. Gan, *RSC Adv.*, 2015, **5**, 59887.
32 A. K. L. Sajjad, S. Shamaila, B. Tian, F. Chen and J. Zhang, *Appl. Catal. B.*, 2009, **91**, 397.
33 X. Z. Li and Y. Q. Wang, *J. Alloys Compd.*, 2011, **509**, 5765.
34 Z. F. Zhang, H. R. Liu and H. Zhang, *Superlattice. Microst.,*2014, **65**, 134.
35 C. G. Tian, W. Li, K. Pan and Q. Zhang, *J. Solid. State. Chem.,* 2010, **183**, 2720.
36 H. Tahiri, Y. A. Ichou and J. M. Herrmann, *J. Photochem. Photobiol. A.*, 1998, **114**, 219.
37 Y. M. Dong, C. Y. Feng and P. P. Jiang, *RSC Adv.* 2014, **4**, 7340.
38 X. X. Lin, F. Rong, D. G. Fu and C. W. Yuan, *Powder. Technol.* 2012, **219**, 173.
39 Y. S. Liu, S. H. Wei and W. Gao, *J. Hazard. Mater.*, 2015, **287**, 59.
40 A. L. Linsebigler, G. Q. Lu and J. T. Yates, *Chem. Rev.*, 1995, 95, 735.
41 Q. Deng and X. W. Duan, *ACS Appl. Mater. Interfaces.* 2012, **4**, 6030.
42 . L. Wang, H. H. Qian and Y. Hu, W. Dai, *Dalton Trans*. 2013, **42**, 1122.
43 X. T. Yin, W. X. Que, Y. L. Liao, H. X. Xie and D. Fei, *Colloids and Surfaces A: Physicochem. Eng. Aspects,* 2012, **410**, 153.
44 Q. Xiao, Z. C. Si, J. Zhang, C. Xiao and X. K. Tan, *J. Hazard. Mater.,* 2008, **150**, 62.
45 Q. J. Xiang, J. G. Yu and P. K. Wong, *J. Colloid. Interf. Sci.*, 2011, **357,** 163.
46 K. Ishibashi, A. Fujishima, T. Watanabe and K. Hashimoto, *Electrochem. Commun.*, 2000, **2**, 207.
47 M. Hsu and C. Chang, *J. Hazard. Mater.,* 2014, **278**, 444.
48 M. Khan, C. S. Wei, M. M. Chen, J. J. Tao and Z. M. Qi, *J. Alloy. Compd.,* 2014, **612**, 306.
49 H. J. Zhai, L. J. Wang, D. W. Sun, J. H. Yang, L. M. Chang and X. F. Li, *Catal. Lett.,* 2015, **145**, 1041.

Graphical Abstract

A series of flower-like Ag/ZnO composites was prepared with various Ag contents by a facile two-step method. The prepared photocatalyst displays excellent photocatalytic activity for Rhodamine B (RhB) under ultraviolet and visible light. And the Ag/ZnO is a promising candidate material for future treatment of contaminated water.